A millimeter wave high isolation resistive coupler In 45nm RFSOI technology for sensing application

Aïcha Saïd, Frédéric Hameau, Rémy Vauché, Alexandre Siligaris, Florence Podevin, Sylvain Bourdel

A Millimeter Wave High Isolation Resistive Coupler In 45nm RFSOI Technology for Sensing Application

Aïcha Saïd[1], Frédéric Hameau[1], Rémy Vauché[2], Alexandre Siligaris[1], Florence Podevin[3], Sylvain Bourdel[3]
[1]Univ. Grenoble Alpes, CEA Leti, 38000 Grenoble, France
[2]Univ. Aix Marseille, IM2NP, 13013 Marseille, France
[3]Univ. Grenoble Alpes, Grenoble INP, TIMA, 38000 Grenoble, France

***Abstract*—This paper proposes the design and test of a high isolation millimeter wave directional coupler for sensing application. The compact device is fabricated using the 45nm RFSOI technology of Global Foundries. The core size of the coupler is 44 µm × 34 µm. An insertion loss close to the expected 3.6 dB and a coupling ratio of about 26 dB within the 40-80 GHz frequency band have been reached. Moreover, the proposed coupler achieved a measured isolation greater than 43 dB at 60 GHz. This performance is particularly mandatory in sensing applications where maintaining the integrity of the measured signal is critical.**

Keywords—Millimeter wave coupler, integrated directional coupler, high isolation coupler, CMOS

I. Introduction

Radiofrequency (RF) directional couplers are essential blocks for many high-frequency applications, including radars, RFID or sensing applications. Among sensing systems, a wide field of wireless sensors is emerging nowadays, based on contactless reflection measurement for the detection of vital signs [1], or cancers [2], and for characterization of chemical, biological or medical liquids [3]. Usually a vector network analyzer (VNA) is used to measure the recovered data. To reduce cost and size, integrated compact systems, which include a directional coupler, have been developed at millimeter wave frequencies. Indeed, working at millimeter wave frequency (around 60 GHz) is a great advantage for integration and opens a large variety of physical parameter to be monitored. For sensing applications, a coupler with a limited isolation can lead to a decrease in system sensitivity, to signal distortion and to a poor dynamic. In practice, high isolation that is 15 dB above coupling is required, leading to an isolation greater than 40 dB for low couplings of about 25 dB. Moreover, at millimeter wave frequencies, the design of integrated couplers with high performances becomes more challenging due to the variations of the manufacturing process, voltages and temperature.

There are several types of integrated RF couplers used at millimeter wave frequencies, including coupled-line directional couplers, branch-lines and bridge couplers. Coupled-line couplers performances are determined by the spacing and the width of the transmission lines. In [4], for example, a differential coupler consists of two broadside coupled transmission lines, showing a low insertion loss and a compact size, but for which width and spacing have huge impact on the behavior. Branch-line couplers rely on four transmission lines, each of a quarter-wavelength at the operating frequency. The performances of these couplers are also depending on the dimensions of the transmission lines and they are known to be narrow-band and to have large size. In [5], authors propose slow-wave transmission lines and prove higher compactness together with extended bandwidth, but at the cost of more insertion loss. By the way, transmission lines based couplers inherently achieve a maximum isolation around 30 dB, [4], [5], [6], [7], due to unavoidable intrinsic parasitic coupling effects. To improve this parameter, several approaches were presented in the literature, most often related to even-odd velocities compensation for coupled lines couplers as in [8] for sub-GHz applications and, [9] at 200 GHz. However, all of them stay far from the targeted isolation.

Resistive couplers, also known as bridge couplers, are a type of RF couplers that use a resistive network to split or combine RF power between two or more ports. As lumped-type circuits, they are much less affected by unwanted coupling effects and can provide excellent isolation performance depending on the choice of the resistance values (higher than 50 dB at 26 GHz, [10]). In addition, these couplers offer wide bandwidth, design simplicity, low-cost fabrication and compact size.

To obtain a high isolation coupler as required by the targeted sensing application, it is proposed in this paper to design a high isolated and integrated resistive coupler optimized at 60 GHz. The paper is organized as follows. A system study for performance requirement analysis is presented in section II. Section III focuses on the architecture and the design of the resistive coupler. Finally, in section IV, simulation and measurement results are shown and validate the coupler performances.

II. Application System Study

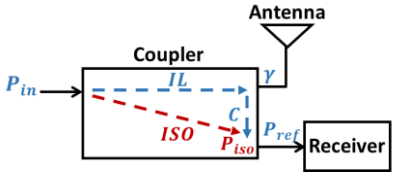

Fig. 1. Simplified block diagram of a sensing system including a coupler

Fig. 1 presents a simplified block diagram of the targeted sensing system including a directional coupler. The coupler provides an isolation between the PA port and the LNA port to prevent the PA signal from leaking into the receiver path and interfering with the received signal coming back from the antenna port. A system study has been carried out to determine the required coupler performances which allow the reflected signal coming from the antenna to be detected by the receiver. The reflected signal P_{ref} and the isolated signal P_{iso} can be expressed as follows:

$$P_{ref} = P_{in} - IL + \gamma - C \quad (1)$$

$$P_{iso} = P_{in} - ISO \quad (2)$$

where P_{IN}, γ, IL, ISO and C are respectively, the power input signal, the antenna reflection coefficient, the insertion loss, the isolation and the coupling ratio of the coupler. By taking

P_{in} = 0 dBm, IL = 3 dB, γ = - 15 dB (S_{11} = - 15 dB, minimum to detect from antenna) and C = 25 dB (to avoid receiver signal saturation), the reflected power P_{ref} is equal to - 43 dBm. To recover the reflected signal correctly an isolation greater than 43 dB at least is necessary to maintain a reflected-to-isolated signal ratio greater than 0 dB.

III. RESISTIVE COUPLER DESIGN

A. Architecture

Fig. 2 shows the used resistive coupler architecture [10]. The device has single-ended input and transmission ports but differential coupled and isolation ports enabling differential receiver feeding.

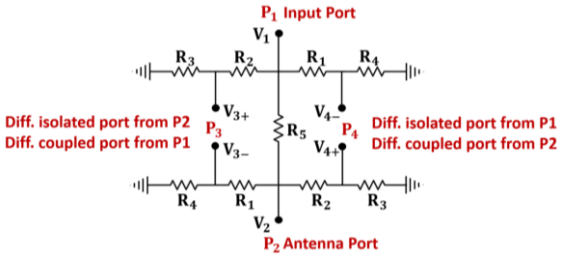

Fig. 2. Schematic of the coupler architecture

Using Kirchhoff's laws, insertion loss (il), coupling (c) and isolation (iso) can be expressed as follows:

$$il = \frac{V_2}{V_1} = \frac{g + \frac{2acd}{be - c^2}}{f - \frac{1}{be - c^2}(bd^2 + ea^2)} \quad (3)$$

$$c = \frac{V_{4+} - V_{4-}}{V_2} = \frac{1}{be - c^2}[a(e - c) + d(c - b)il] \quad (4)$$

$$iso = \frac{V_{4-} - V_{4+}}{V_1} = \frac{1}{be - c^2}[d(b - c) + a(c - e)il] \quad (5)$$

with $a = 1/R_2$, $b = 1/Z_0 + 1/R_2 + 1/R_3$, $c = 1/Z_0$, $d = 1/R_1$, $e = 1/Z_0 + 1/R_1 + 1/R_4$, $f = 1/R_1 + 1/R_2 + 1/R_5 + 1/Z_{\mathrm{DUT}}$, and $g = 1/R_5$, where Z_0 is the differential impedance of isolated and coupled ports, and Z_{ant} is the antenna impedance. Z_0, Z_{ant}, R_1, R_2, R_3, R_4 and R_5 are equal to 100, 50, 196, 144, 288, 235, and 9 Ω respectively theoretically resulting in $IL = -20\,log(il)$= 1,7 dB, $C = -20\log(c)$ = 22 dB and $ISO = -20\log(iso)$ = 62 dB.

The core coupler, i.e. the resistive coupler shown in Fig. 2 including small access lines to poly-resistors, was implemented using the 45 nm RFSOI technology from Global Foundries for an operating frequency of 60 GHz. The core coupler is highlighted in blue in Fig. 3.

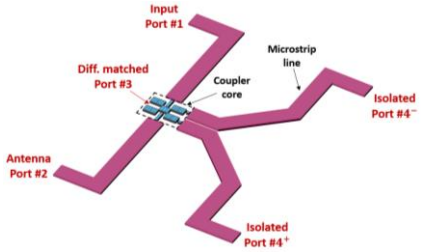

Fig. 3. 3-D view of the fabricated coupler (core coupler in blue and 50 Ω microstrip accesses to be de-embedded in pink. Probe pads are not represented but are de-embedded as well)

Since there is no need for Port 3 in our sensing system, the coupled port (from Port 1 input signal point of view) is not used and is simply differentially terminated with a 100-Ω on-chip resistance. After parasitic extraction, the simulated isolation between Port 1 and Port 4 is about 50 dB, the simulated coupling between Port 2 and Port 4 is close to 27.1 dB and the simulated insertion loss between Port 1 and Port 2 is equal to 3.1 dB.

Resistive couplers are known to be very sensitive to process variations. A Monte Carlo simulation of the core coupler (including small access lines) is performed at 60 GHz to exhibit the sensitivity of the isolation through resistances variation. Fig. 4 shows the Monte Carlo distribution of the isolation performance considering both mismatch and process variations for the post-layout extracted resistances R_1 to R_5. A deviation of about 10 dB is observed on the isolation, which is further considered when designing the coupler.

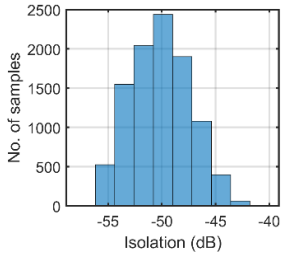

Fig. 4. Isolation value distribution using a Monte Carlo simulation of the core coupler considering mismatch and process variations for the resistances R_1 to R_5

In order to characterize under probe the coupler performances, 50-Ω microstrip lines were implemented to connect the singled-ended input port (Port 1), the single-ended antenna port (Port 2) and the differential Port 4 (between Ports 4^+ and 4^-) to four RF pads as shown in Fig. 3.

An electromagnetic (EM) simulator has been used to simulate the core coupler and the coupler with its 50-Ω accesses lines. Fig. 5 displays a comparison between the simulated coupler S-parameters with and without the access lines. It can be observed that there are some degradations of the isolation parameter. An insertion loss and a coupling of 4.1 dB and 27.8 dB respectively are reached within the frequency band 40-80 GHz. The isolation is only 36.1 dB for the simulated coupler with access lines at 60 GHz. We estimate a 15 dB isolation degradation as compared to the intrinsic isolation due to the impact of access lines parasitic capacitances effects whereas the coupling ratio and the insertion loss are weakly impacted (a few losses added). In the next section, coupler access lines will be de-embed to get the exact performances of the core coupler.

IV. MEASUREMENTS RESULTS

A die micrograph of the proposed on-chip device including the access lines is presented in Fig. 6. The core size of the coupler is 44 µm × 34 µm. The measurements have been carried out using a four-port network analyzer (MS4647B) and two GSGSG-type probes from 40 GHz to 80 GHz. The access lines have been de-embedded enabling to extract their parasitic coupling effect between themselves in order to retrieve the exact isolation. The results are presented in Fig. 7. The de-embedded measurement and the simulated intrinsic results show good agreement within the frequency range 40-80 GHz. A maximum measured insertion loss of

3.6 dB is reached within the frequency span (Fig. 7 (a)). A wideband measured coupling ratio of 26 dB is obtained close to the simulated one (Fig. 7 (a)). A good matching, lower than 12 dB, for Ports 1 and 2, is reached during measurements between 40 GHz and 80 GHz. Moreover, the return loss of the isolated port is close to 10 dB (Fig. 7 (b)). Finally, the measured isolation ratio is about 43 dB at 60 GHz for the de-embedded coupler compared to 50 dB for the simulated intrinsic coupler as it is shown in Fig. 7 (c).

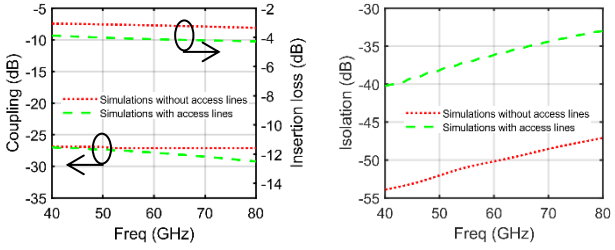

(a) (b)

Fig. 5. Coupling, insertion loss (a) and isolation (b) of the simulated coupler with (green dashed lines) and without (red dot lines) aaccess lines

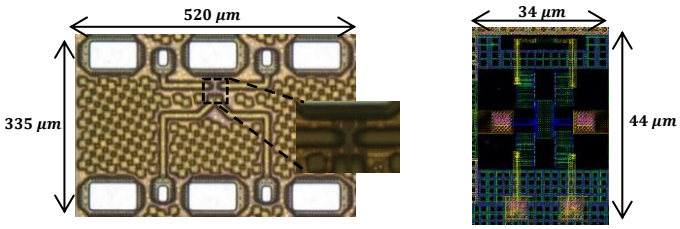

(a) (b)

Fig. 6. Chip micrograph (a) and layout (b) of the proposed coupler

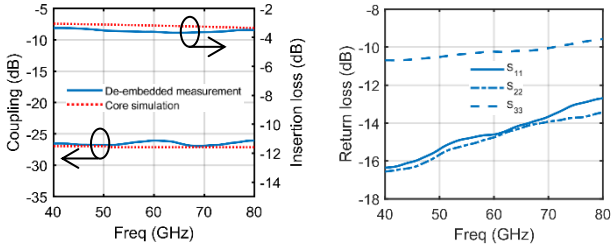

(a) (b)

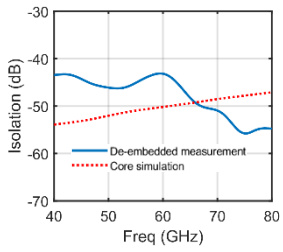

(c)

Fig. 7. Scattering parameters of the de-embedded measured coupler and of the simulated core coupler (EM simulation)

TABLE I. compares the performance of previously reported integrated couplers operating at 60 GHz. The table highlights the good results of the proposed coupler, particularly for isolation performance. Despite proving results very close to the expected simulated ones, our device shows a significant wide band of 40 GHz and a compact size. Clearly, as compared to previous works, our design shows a higher insertion loss (around 3.6 dB) which could be found significant (regarding the low targeted coupling of 26 dB) but that is necessary, authors insist, to prevent signal saturation at the receiver side. In counterpart, for a similar coupling, assuming it can be reached, a distributed coupler would present a typical *IL* of 0.5 to 1 dB only, depending on the transmission lines attenuation loss for the considered technology. This is one drawback of the resistive bridges and the price to pay for an isolation as high as 43 dB.

TABLE I. PERFORMANCE COMPARISON OF 60 GHZ COUPLERS

Ref.	[4]	[5]	[6]	[7]	**This work**
Frequency (GHz)	75	60	60	75	**60**
Process (nm)	28 FDSOI	22 CMOS	130 BiCMOS	350 SiGe	**45 RFSOI**
Architecture	Coupled line	Branch line	Lange line	Coupled line	**Resistive coupler**
Bandwidth (GHz)	21*	24	17	50	**40**
Insertion loss (dB)	0.5*	4.55	4	1.8	**<3.6**
Isolation (dB)	30*	22.3	16	32	**43**
Coupling (dB)	3*	5.35	5	12	**26**
Area (um²)	174×49	300×220	300×160	-	**44×34**

*Simulated

V. CONCLUSION

A directional millimeter wave resistive coupler has been designed and fabricated. The measured coupler achieves a very good isolation, better than 43 dB at 60 GHz with a coupling of 26 dB and 3.6 dB of insertion losses. Moreover, the coupler provides a wide frequency band of 40 GHz. Finally, the measured performances make the coupler a promising candidate for a wide range of sensing applications, where accurate and efficient signal detection is required.

REFERENCES

[1] H. Arab et al., « Early-Stage Detection of Melanoma Skin Cancer Using Contactless Millimeter-Wave Sensors », *IEEE Sensors Journal*, vol. 20, nº 13, p. 7310-7317, 2020

[2] Y. Hong, S.-G. Kim, B.-H. Kim, H.-J. Lee, G.-H. Yun, et J.-G. Yook, « Advanced non-contact near-field proximity vital sign sensor using phase locked loop », *EuMC*, p. 605-608, 2013

[3] M. Hofmann et al., « Microwave-Based Noninvasive Concentration Measurements for Biomedical Applications », *IEEE T-MTT*, vol. 61, nº 5, p. 2195-2204, 2013

[4] F. Voineau et al., « A differential vertical hybrid coupler and low capacitance RF pads for millimeter-wave applications in 28 nm CMOS FDSOI », *IEEE SiRF*, p. 57-59, 2018

[5] G. Acri et al., "A Millimeter-Wave Miniature Branch-Line Coupler in 22-nm CMOS Technology," *IEEE SSCL*, vol. 2, no. 6, pp. 45-48, 2019

[6] M. K. Chirala et B. A. Floyd, « Millimeter-Wave Lange and Ring-Hybrid Couplers in a Silicon Technology for E-Band Applications », *IEEE MTT-S*, p. 1547-1550, 2006

[7] I. Nasr et al., « Single- and Dual-Port 50-100-GHz Integrated Vector Network Analyzers With On-Chip Dielectric Sensors », *IEEE T-MTT*, vol. 62, nº 9, p. 2168-2179, 2014

[8] R. Islam et al., « Printed high-directivity metamaterial MS/NRI coupled-line coupler for signal monitoring applications », *IEEE MWTL*, vol. 16, nº 4, p. 164-166, 2006

[9] M. Margalef-Rovira et al., "Design of mm-Wave Slow-Wave-Coupled Coplanar Waveguides," *IEEE T-MTT*, vol. 68, no. 12, pp. 5014-5028, 2020

[10] H. Chung et al., « A Packaged 0.01–26-GHz Single-Chip SiGe Reflectometer for Two-Port Vector Network Analyzers », *IEEE T-MTT*, vol. 68, nº 5, p. 1794-1808, 2020